Journal of Sea Research
November 2013, volume 84, Pages 109-121
http://dx.doi.org/10.1016/j.seares.2012.12.005

Spatial variation in growth, maturation schedules and reproductive investment of female sole Solea solea in the Northeast Atlantic

Fabian M. Mollet[a, b, 1, *], Georg H. Engelhard[c], Anssi Vainikka[d, 2], Ane T. Laugen[e], Adriaan D. Rijnsdorp[a, f], Bruno Ernande[g, h]

[a] Wageningen Institute for Marine Resources and Ecosystem Studies (IMARES), P.O. Box 68, 1970 AB IJmuiden, The Netherlands
[b] Evolution and Ecology Program, International Institute for Applied Systems Analysis, Schlossplatz 1, A-2361 Laxenburg, Austria
[c] Centre for Environment, Fisheries and Aquaculture Science (Cefas), Pakefield Road, Lowestoft NR33 0HT, UK
[d] Institute of Coastal Research, Swedish Board of Fisheries, Öregrund, Sweden
[e] Swedish University of Agricultural Sciences, Department of Ecology, Box 7044, 75007 Uppsala, Sweden
[f] Aquaculture and Fisheries group, Wageningen University, P.O. Box 338, 6700 AH, Wageningen, The Netherlands
[g] IFREMER, HMMN, Laboratoire Ressources Halieutiques, F-62200 Boulogne-sur-Mer, France
[h] Univ Lille Nord de France, F-59000 Lille, France

[1] Present address : Blueyou Consulting Ltd, Zentralstrasse 156, 8003 Zürich, Switzerland
[2] Present address : Department of Biology, University of Eastern Finland (P.O. Box 111, FI-80101 Joensuu, Finland).

*: Corresponding author : Fabian M. Mollet, email address : fabian.mollet@blueyou.com

Abstract:

Latitudinal variation in life-history traits is often explained by phenotypically plastic responses or local adaptations to different thermal regimes. We compared growth, maturation schedules and reproductive investment of female sole *Solea solea* between 8 populations, covering much of the species' distribution in northern Europe, with respect to thermal gradients. An energy allocation model was fitted to size–age data, and probabilistic maturation reaction norms were estimated from size–age–maturity data. We found that northern populations from colder environments had higher rates of energy acquisition and reproductive investment, an intrinsic tendency to mature earlier, and had smaller asymptotic sizes than southern populations from warmer environments. Consequently, growth rate was higher before maturation but lower after maturation in the north compared to the south. This is opposite to Bergmann's rule according to which slower growth, delayed maturation and larger asymptotic sizes are usually observed at lower temperatures. The observed patterns could indicate strong countergradient thermal adaptation for rapid growth and development as well as sustained fecundity in the north, or indicate a response to other selection pressures correlated with the thermal gradient. Potentially higher mortality in northern populations during cold winters might be one of the key drivers of the observed geographical variation in growth and maturation of sole.

Highlights

► Fishery data from three renown research institutions have been combined. ► A novel methodology is used to simultaneously estimate multiple life history traits. ► Plasticity and local adaptation are evaluated as response to the temperature gradient. ► Findings are opposite to Bergmann's rule indicating countergradient variation. ► Differences in natural mortality seems the main cause for life history adaptation.

Keywords: Countergradient variation ; Phenotypic plasticity ; Growth ; Maturation reaction norm ; Temperature ; Mortality-induced evolution

Introduction

Adaptation along thermal gradients

The ecological and evolutionary processes behind latitudinal variation in phenotypes have captured the attention of biologists for a long time, but in many cases the relative importance of these processes remains unclear. With increasing human interference on ecosystems and corresponding demands for assessment and mitigation of its consequences, it is urgent to estimate the causes and magnitude of naturally occurring as well as human-induced processes together with their interactions (Conover and Schultz, 1995, Conover et al., 2009).

Environmental heterogeneity in biotic or abiotic factors often changes gradually with latitude, and one of the most studied drivers of latitudinal clinal variation is temperature. Several biogeographical rules have been put forth to explain temperature-driven phenotypic patterns, one example being Bergmann's rule (Bergmann, 1847). This rule, originally applied to endotherms and mostly observed in birds and mammals (Blackburn and Hawkins, 2004), asserts that body size within species increases with latitude and colder climate, or that within closely related species differing mainly in relation to size, one would expect the larger species to be found at the higher latitude. This pattern may be explained by the lower surface to volume ratio of the larger body size if the dissipation of thermal energy is costly (colder environments), or by the higher surface to volume ratio of smaller body size if the accumulation of surplus thermal energy is costly (warm environments). The application of Bergmann's rule to ectotherms has yielded mixed results; depending on the species researches have reported Bergmann size patterns but also its reverse, known as Converse Bergmann's rule (Angilletta et al., 2004; Mousseau, 1997; Litzgus et al., 2004; Blanckenhorn and Demont, 2004; Conover et al., 2009).

One key question in studies of latitudinal clines is to assess if the observed phenotypic variation results from phenotypic plasticity, local adaptation or both (Arendt, 1997; Conover et al., 2009; Partridge and Coyne, 1997; Van Voorhies, 1997). Experimental assessments of phenotypic plasticity generally show that lower temperatures reduce developmental rates more than growth rates resulting in larger sizes at a given developmental stage such as metamorphosis or maturation (Angilletta, 2008). This causality corresponds to Bergmann's rule and may be referred to as the temperature-size rule. This plastic response may have a genetic basis (coined as genotype by environment interaction; Lynch and Walsh 1998), and it often varies between populations of the same species (Laugen et al., 2003, 2005). A phenotypic pattern corresponding to the plastic response of a trait to differences in temperature along the spatial gradient is expected if there is no genetic variation along this gradient in this trait (hypothesis H1, Fig. 1A).

Besides phenotypic plasticity, two different patterns of genetic variation due to local adaptation can also affect latitudinal phenotypic clines (Fig 1; Conover and Schultz, 1995; Conover et al., 2009). Cogradient variation (CoGV; hypothesis H2, Fig. 1B) is expected if adaptive genetic variation is in the same direction as plastic variation along the gradient. Since genetic and plastic variation cumulate in the phenotypic response, the pattern of the temperature effect on a trait along the gradient is then reinforced (Trussell, 2000; Conover et al., 2009). The other pattern, countergradient variation (CnGV; hypothesis H3, Fig 1C), is expected if the direction of environmentally induced plastic variation is maladaptive in the sense that it is opposite to the expected adaptive response along the gradient. This may occur for instance in case of passive plastic responses arising from pure physical laws (e.g. warmer temperatures increase chemical reaction rates). This implies that adaptive genetic variation opposes plastic variation (Trussell, 2002; Skelly, 2004; Schultz et al., 1996; Marcil et al.,

2006; Conover et al., 2009; Conover and Present, 1990; Blanckenhorn and Demont, 2004). CnGV dampens the effect of plasticity in phenotypic variation, and typically results in a flat phenotypic pattern (Fig. 1C) that thus conceals substantial amounts of genetic variation among populations (see e.g. Laugen et al., 2003). CnGV in growth has been detected mostly in fishes, amphibians and insects (Conover et al., 2009; Conover and Present, 1990; Marcil et al., 2006; Lonsdale and Levinton, 2011; Lindgren and Laurila, 2010; Schultz et al., 1996).

Both CoGV and CnGV can be detected by common garden experiments in which the expression of traits is compared between individuals from different origin (Blanckenhorn and Demont, 2004; Arnett et al., 1999; Conover and Present, 1990; Laugen et al., 2003; Lindgren and Laurila, 2005; Marcil et al., 2006; Schultz et al., 1996). Reaction norm-based statistical approaches, which are able to approximate the genotypic value of traits by combining phenotypic and environmental field data (see e.g. Heino et al., 2002), could also be used for detecting CoGV and CnGV. Here we combine energy allocation modelling together with a reaction norm-based analysis of maturation to study phenotypic latitudinal clines in life-history traits (energy acquisition, growth rate, reproductive investment, age and size at maturation) and, to our knowledge, are the first ones to apply such an approach.

Life history and energy allocation

Life history traits are correlated both genetically and phenotypically, which is challenging for studying life-history adaptation. Phenotypic variation across environments, be it from genetic and/or plastic origin, in the allocation of resources to growth and reproduction may maximize individuals' fitness in the environment they experience (Stearns, 1992; Roff, 1992). Since some energy is channelled towards reproduction after maturation, less energy becomes available to growth. Growth rate is thus expected to decrease discontinuously at maturation (West et al., 2001). Through modelling of energy allocation, the shape of an individual's

growth curve therefore informs about the onset of maturation and reproductive investment (Mollet et al., 2010; Brunel et al., in press).

The likelihood of maturation across different environments is conveniently illustrated by the probabilistic maturation reaction norm (PMRNs, Heino et al., 2002). Reaction norms in general describe how a certain genotype is translated into different phenotypes depending on environmental conditions. PMRNs in particular depict how individuals' maturation probability varies with age and size conditional on individuals being still immature and having survived and grown until these age and size. The most important determinant for maturation is likely growth rate (Bernardo, 1993), and PMRNs disentangle plastic variation in maturation probability under the assumption that environmental variability affects maturation through its effect on growth rate. Energy-allocation modelling and PMRNs are therefore both powerful tools to assess life-history traits by simultaneously capturing the inherent correlations among these traits and disentangling plastic and genetic variation. Their application requires age, size and maturity data (and may be extended to incorporate any other environmental or environmentally driven variables).

Sole

Here we study geographic patterns of variation in growth, maturation schedules and reproductive investment of the common sole (*Solea solea*). This is an important commercial species in waters down to about 60 m and targeted in demersal mixed fisheries (Millner et al., 2005). Its distribution ranges from the Mediterranean and north-west coast of Africa in the south to the Irish Sea and the southern coast of Norway and the Kattegat in the north. Genetic differentiation has been shown among Atlantic populations and between the Atlantic and the Mediterranean (Exadactylos et al., 2003; Cuveliers et al., 2012). Synchronous variations in recruitment, however, occur at a much smaller spatial scale and support the interpretation that

ICES management areas (ICES, 2010) represent distinct biological stocks, although within the North Sea for instance there are more sub-stocks present (Fig. 2, Rijnsdorp et al., 1992). Growth rates in the Atlantic Ocean are higher than in the North Sea and the Mediterranean (Deniel, 1981; Horwood, 1993). There are also clear geographical patterns of variation in the fecundity–size relationship, egg size and timing of the spawning period (Witthames et al., 1995; Rijnsdorp and Vingerhoed, 1994; Fincham et al., 2013). These patterns may be related to a gradient in fecundity-regulating mechanisms changing from determinate fecundity type in the early spawning southern populations to indeterminate fecundity type in the later spawning northern populations (Rijnsdorp and Witthames, 2005).

Contribution of this study

In this paper we take a novel approach to latitudinal life-history clines by using an energy allocation model together with PMRNs to analyze how growth, maturation and reproductive effort in female sole vary along a latitudinal gradient in relation to temperature as an environmental factor of primary importance. From the observed population differences in growth, maturity and reproduction we evaluate if these differences are due to (H_1) a plastic response to temperature or (H_2) local adaptation generating CoGV, consistent with Bergmann's rule (Atkinson and Sibly, 1997), with warmer temperatures inducing faster growth, earlier maturation and smaller asymptotic sizes, or (H_3) local adaptation creating CnGV, i.e. genetic variation opposite to the plastic response.

Materials and Methods

Data sources and populations

The data cover biological samples from eight populations distributed between the Bay of Biscay in the south and the Irish Sea and North Sea in the north (Fig. 2). A total of 56380 females were sampled from scientific survey catches and commercial landings according to a length-stratified design during the period 2000-2005 (Table 1). Three research institutes contributed to the data set: Cefas (England) covering the North Sea (management area IVb east, IVb west, and IVc), the Irish Sea (management area VIIa), the Channel (management areas VIId and VIIe) and the Celtic Sea (IVfg); IFREMER (France) covering the Channel (management area VIId and VIIe) and the Bay of Biscay (management area VIIIa); and IMARES (The Netherlands) covering the North Sea (management area IVc, IVb west, IVb east).

For each female the following data were available: sampling date (day, month, year), age (years; determined by otolith reading assuming the 1st of January as birth day), length (cm), weight (g) and, for a subset of 15266 females, maturity stage (Mollet et al., 2007). Maturity stage was determined by visual inspection of the gonads. Although detailed maturity staging was not standardized among the three institutes, the distinction between immature and mature females was carried out in a comparable manner. Age was transformed to a continuous variable by accounting for the moment of sampling within a year. Since there is variation in the onset of spawning among stocks, continuous age was additionally corrected for the reported peak of spawning of each stock (Arbault et al., 1986; Fox et al., 2000; Rijnsdorp and Vingerhoed, 1994).

No comparable measures of bottom temperature were available for all areas. Therefore, we

used bottom temperatures from the bio-physical models NORWECOM (Søiland and Skogen, 2000) for areas north of 48°N and MARS3D (Huret et al., 2013) for area VIIIa. The mean bottom temperature was estimated for each management area for the depth zone 10-50 m for the period 1985-2008 and taking account of the surface of each depth layer. These weighted means were then averaged by month over the period 1985-2008 to obtain relatively robust monthly temperature indices per area $\overline{T}_{m,z}$ (m month, z area; see Fig. 3).

Growth and energy allocation

Energy-allocation based growth model

Growth and underlying bioenergetics are studied using an energy allocation model, in which the change $\partial w/\partial t$ in somatic weight w according to time t, i.e. age, is given by the difference between energy acquisition and energy expenditure :

$$\frac{\partial w}{\partial t} = aw^{\alpha} - cw \qquad (1)$$

where aw^{α} is the rate of net energy acquisition that scales with somatic weight to the power of α with size-specific rate a and cw is the rate of reproductive investment scaling with somatic weight to the power of 1 with size-specific rate c. We assume $\alpha = 0.75$ which seems a good approximation in general (West et al., 2001) and in flatfish in particular (Fonds et al., 1992; Mollet et al., 2010). Juveniles do not expend energy for reproduction and hence $c = 0$, whereas after the onset of maturation at age t_{mat} acquired energy is shared between growth and reproduction, so that $c > 0$. In this model, energy expenditure for maintenance is accounted for by the size-specific acquisition rate, i.e. a is the size-specific rate of energy inflow that remains after first meeting the energy requirements for maintenance. This implies that the rate of absolute energy acquisition and the rate of expenditure for maintenance scale

equally with body weight (see e.g. Lester et al., 2004). Variation in size-specific net energy acquisition rate a thus results from a combination of variation in size-specific absolute energy acquisition rate and size-specific maintenance rate. These considerations are important for interpretation because differences in a across stocks may not only result from differences in size-specific absolute energy acquisition rate but also in size-specific maintenance rate.

By integration of eq. (1), juvenile ($c = 0$) and adult ($c > 0$) growth curves describing somatic weight as a function of age are obtained. An individual starts to grow following juvenile growth until it matures and switches to the adult curve because of energy expenses for reproduction. A single lifetime growth curve is obtained by combining juvenile and adult growth functions using the Heaviside step function, $H_{t_{\mathrm{mat}}}(t)$ ($H_{t_{\mathrm{mat}}}(t) = 0$ for $t < t_{\mathrm{mat}}$ and $H_{t_{\mathrm{mat}}}(t) = 1$ for $t \geq t_{\mathrm{mat}}$), to describe the switch between one curve to another occurring at the onset of maturation t_{mat} corresponding to the size at maturation w_{mat}:

$$w^{1-\alpha}(t) = (1 - H_{t_{\mathrm{mat}}}(t))\left[w_0^{1-\alpha} + a(1-\alpha)t\right] + H_{t_{\mathrm{mat}}}(t)\left[\frac{a}{c} - \left(\frac{a}{c} - w_{\mathrm{mat}}^{1-\alpha}\right)\mathrm{e}^{-c(1-\alpha)(t-t_{\mathrm{mat}})}\right] \quad (2.1)$$

with w_0 being the somatic weight at birth of an individual assumed to be constant across populations at 2.5 mg (Mollet et al., 2010).

The three energy allocation parameters a, c, and w_{mat} were estimated by fitting equation (2.1) to age-at-somatic weight data. Somatic weight of an individual varies seasonally in relation to the energy reserves and gonad weight. To avoid the risk of confounding between weights of different compartments due to variable body condition when using total weight, length records were transformed to somatic weight by using a length-weight relationship (see

231 eq. 6 below) evaluated at the seasonal minimal average body condition in each management
232 area.

233 The available weight-at-age data are biased and not representative of the population because
234 of (i) the length stratified sampling design and (ii) truncation of the size distribution due to
235 the mesh size used (research vessel survey samples) and the minimum landing size
236 (commercial samples). In contrast, sampling and fishing are not selective for age (conditional
237 on size), and we can therefore assume that our samples provide representative age
238 distributions within a size class. By fitting the growth model to age-at-somatic weight instead
239 of somatic weight-at-age data, the sampling bias described above can be avoided. Growth
240 function (2.1) was inverted to obtained age t as a function of somatic weight w using a size-
241 $S(w-w_{\text{mat}})$ instead of an age-dependent Heaviside step function:

242 $$t(w) = (1 - H_{w_{\text{mat}}}(w))\left[\frac{1}{a(1-\alpha)}(w^{1-\alpha} - w_0^{1-\alpha})\right] + H_{w_{\text{mat}}}(w)\left[t_{\text{mat}} - \left(\frac{1}{c(1-\alpha)}\log\left(\frac{a/c - w^{1-\alpha}}{a/c - w_{\text{mat}}^{1-\alpha}}\right)\right)\right] \quad (2.2)$$

243 ***Growth model fitting***

244 Nonlinear mixed effect modelling (NLME) was used to fit the inversed energy allocation
245 model (2.2) to age-at-somatic weight data. Following Pinheiro and Bates (2004), the NLME
246 model was formulated as

247 $$\ln(1 + t_{i,w,z}) = \ln(1 + t(w, \boldsymbol{\mu}_z)) + \varepsilon_{i,w,z} \quad (3)$$

248 where $t_{i,w,z}$ is the age of individual i having somatic weight w in management area z,
249 $t(w, \boldsymbol{\mu}_z)$ is the inverted growth model given in equation (2.2) with $\boldsymbol{\mu}_z = (a_z, c_z, w_{\text{mat},z})^{\text{T}}$ the
250 vector of energy allocation parameters to be estimated for management area z (with bold
251 denoting vectors or matrices and T transpose), and $\varepsilon_{i,w,z}$ is a normally distributed residual

term. Data were ln+1-transformed to achieve normality of the residuals and a residual variance function with differing variances for each management area was included in the model to account for heteroscedasticity of residuals across areas.

To evaluate variation in the three energy allocation parameters across management areas areas and its potential relationship with latitude or temperature, the vector of parameters $\boldsymbol{\mu}_z$ was described as the sum of a vector of fixed effects representing energy allocation parameters as linear functions $\boldsymbol{\mu}(x_z) = (a_0 + a_1 x_z, c_0 + c_1 x_z, w_{\text{mat},0} + w_{\text{mat},1} x_z)^{\text{T}}$ of the relevant covariate x_z, i.e. either the average latitude Lat_z or the average temperature $\overline{T}_z$ in each management area, plus a vector of random effects $\boldsymbol{\Delta\mu}_z = (\Delta a_z, \Delta c_z, \Delta w_{\text{mat},z})^{\text{T}}$ corresponding to the deviation of parameters in management area z relative to the prediction of the fixed effect linear model. Parameters in each management area z were thus estimated as

$$\boldsymbol{\mu}_z = \boldsymbol{\mu}(x_z) + \Delta\boldsymbol{\mu}_z = (a_0 + a_1 x_z + \Delta a_z, c_0 + c_1 x_z + \Delta c_z, w_{\text{mat},0} + w_{\text{mat},1} x_z + \Delta w_{\text{mat},z})^{\text{T}} \quad (4)$$

where $\Delta\boldsymbol{\mu}_z$ follows a multivariate normal distribution with mean vector $\mathbf{0}$ and a symmetric covariance matrix $\boldsymbol{\Sigma}^2$ ($\Delta\boldsymbol{\mu}_z \sim \text{MVN}(\mathbf{0}, \boldsymbol{\Sigma}^2)$ and $\boldsymbol{\mu}_z \sim \text{MVN}(\overline{\boldsymbol{\mu}}, \boldsymbol{\Sigma}^2)$.

To estimate variation in energy allocation parameters across areas without any hypothesis about its cause, we started by fitting a simple "area random effect model" by setting covariate x_z to 0, variation being then represented by the area random effects $\Delta\boldsymbol{\mu}_z$ only. The estimation algorithm requires providing starting values for fixed effect parameters. Because of potential divergence depending on initial values, the model was repeatedly fitted over a grid of starting values and the solution with the highest maximum likelihood was selected. In a second step, the effects of latitude and temperature on energy allocation parameters were

tested by fitting successively a "latitude effect model" and a "temperature effect model" by respectively setting x_z to the average latitude and the average temperature in each management area. The latitude and temperature effect models were initially adjusted with a symmetric covariance matrix $\mathbf{\Sigma^2}$ describing the random component of the model as in the area random effect model. As inclusion of covariates in the fixed component was supposed to account for at least part of the observed variation in energy allocation parameters across areas, the random component structure of the model was then simplified using maximum likelihood ratio tests between nested models obtained by either simplifying the covariance structure (e.g. from a symmetric to a diagonal matrix) or by removing random effects on some or all parameters (Pinheiro and Bates 2004). Once the random component structure was selected, the effects of covariates on the fixed component were tested by asymptotic t-tests (Pinheiro and Bates 2004). All latitude and temperature effect models were adjusted using the initial values selected when fitting the area random effect model to obtain comparable results. The relative merits of the three models (area random effect, latitude effect and temperature effect) were evaluated by comparing the final models after selection on the basis of the Akaike Information Criterion (AIC).

Beyond the three energy allocation parameters, additional parameters were indirectly estimated: the onset of maturation in area z estimated as $t_{\text{mat},z} = t(w_{\text{mat}}, \boldsymbol{\mu}_z)$, the asymptotic somatic weight obtained as $w_{\infty,z} = (a_z / c_z)^{1/(1-\alpha)}$, and somatic weight at different ages t calculated as $w_{t,z} = w(t, \boldsymbol{\mu}_z)^{1/(1-\alpha)}$ according to equation (2.1). Standard errors of directly and indirectly estimated parameters were estimated by bootstrapping with 500 repetitions. NLME models were fitted using the nlme package (Pinheiro et al., 2011) of the statistical software R (R Development Core Team 2011).

Maturation

Because individuals have different schedules for the start of vitellogenesis and because spent and immature ovaries are sometimes difficult to distinguish it was recommended to study the maturation characteristics prior to spawning as soon as the probability to detect maturity (or as vitellogenesis had started) is high (Mollet et al., 2007). As the spawning seasons differ between populations (Fig. 7 , Rijnsdorp and Vingerhoed, 1994), we determined specific sampling periods for each population based on the seasonal cycle in body condition. It is well established that the seasonal cycle in body condition reflects the seasonal pattern in feeding and spawning. Body condition is built up during the feeding period, while a minimum condition occurs immediately after fish have reproduced (Rijnsdorp, 1990; Deniel, 1981). Body condition was modelled according to the following seasonal weight-length-relationship:

$$\ln(w_{l,m}) = \beta_0 + \beta_1 m + \beta_2 m^2 + \beta_3 m^3 + \beta_l \ln(l) + \varepsilon_{l,m} \quad (5)$$

where $w_{l,m}$ is gutted weight (including gonads), l is length (cm), m is month in the year, $\varepsilon_{l,m}$ is a normally distributed residual term, and the β's are the parameters of the model.

The duration of spawning was approximated by the difference between the estimates for peak spawning taken from literature (Arbault et al., 1986; Fox et al., 2000; Rijnsdorp and Vingerhoed, 1994) and the spawning low or end of spawning derived from the minimal annual condition (see eq. 5 above, Fig. 3). To analyze maturation, we selected data from the 5 months prior to the expected spawning peak of the corresponding stocks. Model (5) was also used to estimate somatic weight used for fitting the inverted growth model (2.2) (see Section "Growth and energy allocation model" above).

Maturity ogives according to age (i.e., maturity probability-at-age ; see Table 1) are biased

because they do not account for growth plasticity and survival probability. To account for this, probabilistic maturation reaction norms (PMRNs) were used to describe the probability of an immature individual to become sexually mature as a function of its age and size (and thus of the effective growth rate) conditional on surviving until that age and size (Heino et al., 2002). For each area, the probability of being mature $o(t,l)$ as a function of age t and length l was estimated from individual maturity data by logistic regression according to the following linear predictor model:

$$\text{logit}(o_{t,l}) = \beta_0 + \beta_t t + \beta_l l + \beta_{t,l} t \times l \quad (7)$$

where $o_{t,l}$ is the proportion of mature fish per age and length class, t is continuous corrected age (yr), l is length (cm), and the β's are the parameters of the model. As first time spawners in sole cannot be distinguished from repeat spawners, the probability of becoming mature $p(t,l)$ at a certain age t and length l was calculated from the probability of being mature $o(t,l)$ at those age and length minus the probability of being already mature one year before $o(t-1,l-\Delta l)$, conditional on the probability of being immature in the previous year $1-o(t-1,l-\Delta l)$ while accounting for the length increment (Δl)from age $t-1$ to t (Barot et al., 2004):

$$p(t,l) = \frac{o(t,l) - o(t-1,l-\Delta l)}{1 - o(t-1,l-\Delta l)} \quad (8)$$

We assumed that the growth rate and mortality rate at a certain age and size are the same for immature and mature individuals. Although this may not be true in reality, the method is robust to the relaxation of this assumption (Barot et al., 2004). $L_{P50}(t)$ is used to denote the length at a given age t at which the probability of becoming mature is 50%. Estimation of length increments was based on the fitted growth curves previously estimated (eq. 2, see

above). To obtain confidence intervals of the L_{P50} values, the original data set was bootstrapped for each area with 10^4 repetitions.

Differences in PMRN between the areas, i.e. in L_{P50}-at-age, were tested using a randomization approach. For this purpose, each data point was randomly allocated to a management area irrespective of its geographical origin while respecting the same sample sizes per area as in the original dataset, thus randomizing data across management areas. From this randomized data set, PMRNs in each area and differences in L_{P50}-at-age between areas were calculated. This procedure was repeated 10^4 times. To assess how likely the observed differences between areas might have arisen only by chance, the p-value of the randomization test was given as the proportion of randomized samples for which the differences in L_{P50}-at-age were equal to or greater than the observed differences.

Finally, the respective effects of latitude and temperature on the onset of maturation were tested by regressing $L_{P50}(t)$ against the average latitude and the average temperature in each management area. Regressions were weighted by the inverse of the bootstrapped variances to give more weight to better estimated $L_{P50}(t)$.

Results

The average bottom temperature decreased with latitude (Pearson's correlation, $r_p = -0.95$, $p < 0.0005$), whereas the amplitude between minimal and maximal annual temperature increased ($r_p = 0.71$, $p = 0.047$; Fig. 3). The populations at lower latitudes living in warmer conditions started spawning earlier than stocks at higher latitudes ($r_p = 0.93$, $p < 0.001$), and also spawned for longer periods as was suggested by the approximated end of spawning (date of minimal condition) ($r_p = -0.81$, $p = 0.014$; Fig. 3). Earlier spawning correlated with higher

average temperature (r_p = –0.91, p = 0.001) and longer spawning duration correlated with smaller intra-annual variation in temperature (r_p = 0.75, p = 0.030).

The three growth models (the area random effect model, the latitude effect model and the temperature effect model) fitted very well age-at-size data (see Fig. 4 with the temperature effect model as an example). The area random effect model detected significant variation in energy acquisition rate a, reproductive investment rate c, and size at maturation w_{mat} across sole populations (Likelihood Ratio Tests (LRT) between complete model and model excluding random effect on a: $\chi^2_3 = 94.03$, p< 0.001; c: $\chi^2_3 = 95.39$, p<0.001; and w_{mat}: $\chi^2_3 = 151.66$, p<0.001; see population-specific values of $\boldsymbol{\mu}_z = \bar{\boldsymbol{\mu}} + \Delta\boldsymbol{\mu}_z$ in Table 2). The latitude and the temperature effect models that included a linear dependency (eq. 4) of growth parameters (eq. 2.2) on latitude or temperature resulted in a better (lower) AIC than the model area random effect (Table 3), with a clear advantage for the temperature effect model over the latitude effect model. The linear latitude or temperature effects were significant for all parameters (Table 4) and explained varying parts of the variation detected across areas depending on the parameter considered. Variance in reproductive investment c and related co-variances with the other parameters was not significant (LRT: $\chi^2_3 = 4.23$, p=0.238 and $\chi^2_3 = 2.41$, p=0.491 for the latitude and temperature model, respectively); variance in energy acquisition rate a was significant (LRT: $\chi^2_2 = 807.18$, p<0.001 and $\chi^2_2 = 764.44$, p<0.001, respectively) but decreased by 92.5% and 91.5% respectively; and variation in size at maturation w_{mat} was significant (LRT: $\chi^2_2 = 978.04$, p<0.001 and $\chi^2_2 = 849.39$, p<0.001, respectively) and decreased by 1.5% and 18% respectively. Moreover, for the temperature effect model, the covariance matrix of random effects $\boldsymbol{\Sigma}^2$ could be simplified to a diagonal

matrix indicating that a linear temperature effect explained most of co-variation between energy acquisition and size at maturation across areas (LRT between model with and without covariance: $\chi_1^2 = 0.00$, p=1). Since the temperature effect model had the highest likelihood and the lowest AIC, the following results mainly focus on the temperature effect model (see eq. 5).

The size-specific life-history estimates showed a clear spatial pattern: rates of energy acquisition a and reproductive investment c decreased with increasing temperature (increased with increasing latitude), whereas the onset of maturation (size w_{mat} or age t_{mat} at maturation) was delayed at warmer temperature (precocious at higher latitude, Fig. 5). Temperature increase led to a greater proportional decrease in energy acquisition a than in reproductive investment c, as measured by the ratios between their respective slopes and intercepts (Table 4). As a result the asymptotic weight $w_\infty = (a/c)^4$ increased with increasing temperature (and decreased with increasing latitude, Fig. 6, Table 2).

In summary, sole at lower temperatures in the north grew faster, matured earlier, invested more into reproduction, and reached a smaller asymptotic size. As a consequence growth curves differed across populations between juvenile and adult stages: juvenile size-at-age was larger at lower temperatures in the north whereas adult size-at-age was larger at higher temperatures in the south (Fig. 4 and 6). Since the majority of sole have matured by age 3 in all but one of the populations (see maturity probability-at-age in Table 1 and t_{mat} in Table 2), the trend in size-at-age with temperature already started to reverse at age 3 (Fig. 6).

The eight sole populations showed variable probabilistic maturation reaction norm (PMRN) shapes, with PMRN midpoints (or L_{P50}) that either decreased with age (such as in area 8a) or

slightly increased with age (such as in area 7fg, Fig. 7). As a result, the relationships of L_{P50} with temperature or latitude depended on the age group considered. For age groups 2 to 4 across which about 90% of individuals mature, L_{P50} tended to increase with increasing temperature (decrease with increasing latitude, Fig. 8). For age 3 when most individuals spawn for the first time, the regression on temperature was significant at a level of α=0.103, for latitude at a level of α=0.025. The maturation probability at a certain size and age was thus higher in the north than in the south, implying that maturation occurs on average earlier in the north, where temperatures are lower, than in the south, where temperatures are higher. Randomization tests (10^4 replicates) performed for age 3 showed that most of the pairwise differences in L_{P50} between areas were significant except for the following groups of populations: 1) 7a, 7e & 4c; 2) 7a & 4bE; 3) 4bW & 7d (Table 5).

Discussion

Main findings

We examined a set of biological traits in eight sole populations experiencing different temperature conditions along a latitudinal gradient. Comparison of energy allocation models fitted to different populations revealed that northern, cold-water populations were characterized by faster energy acquisition rates, earlier onset of maturation at smaller sizes, higher reproductive investment, and lower asymptotic weights. PMRNs – which, by controlling for differences in growth rate, can be interpreted as an approximation of the genotypic value of maturation probability under the assumption that most plastic variation in maturation age and size originates from variation in growth – furthermore revealed that at a given age and size, fish of northerly populations were more likely to commence reproduction

than fish in southerly populations (i.e. had lower reaction norm midpoints or L_{P50} values). Can the observed differences be attributed to phenotypic plasticity or are populations locally adapted to their specific environmental conditions?

Plasticity *vs.* local adaptation to temperature

The observed pattern is in line with Converse Bergmann's rule, according to which individuals in the north grow to smaller asymptotic size, and contrasts experimental results showing that phenotypic plasticity accelerates growth rates and maturation in warmer environments (Angilletta, 2008). Under hypothesis H_1 assuming phenotypic plasticity in response to temperature as bare cause of variation, cold conditions are expected to lead to slow energy acquisition rate and thus reduced immature growth rate (e.g. Toresen, 1990; Grift et al., 2003; Abookire and Macewicz, 2003; Brander, 2007, Fig. 1A), later onset of maturation (e.g. Jørgensen, 1990; O'Brien, 1999; Engelhard and Heino, 2004), lower reproductive investment, and higher asymptotic weight (Rijnsdorp, 1990; Roff, 1992; Abookire and Macewicz, 2003; Brunel and Dickey-Collas, 2010). No change in the PMRN would be expected since the PMRN concept assumes that environmental variation only directly impacts growth rates (Heino et al., 2002; see also Vainikka et al., 2009). The patterns observed here are thus opposite to those expected from phenotypic plasticity. Since CoGV as assumed in hypothesis H_2 would reveal the same life-history pattern along the gradient as the bare effect of plasticity (Fig. 1B), it can be excluded likewise that the studied sole populations were subject to CoGV.

In contrast, the observed patterns might be in line with hypothesis H_3 assuming local adaptation generating countergradient genetic variation (CnGV), opposite to the phenotypically plastic response (Fig. 1C). In case of CnGV, it is usually observed that

populations living in colder environments show similar energy acquisition rates compared to populations in warmer environments (Conover and Present, 1990). In theory, very strong CnGV in energy acquisition, and resulting growth rate, may overcompensate for the plastic decrease in energy acquisition at lower temperatures and lead to size patterns complying with Bergmann's rule, i.e. larger sizes at higher latitudes and colder environments (Conover et al. 2009). This is precisely what we observed for juvenile size-at-age. Local adaptation may also have occurred in maturation generating again CnGV. PMRN midpoints increased with increasing temperature (decreased with increasing latitude) which can be interpreted as CnGV compensating for delayed maturation expected from the plastic decrease in growth rate in colder environments (see also Vainikka et al. 2009). Finally, the observed increase of reproductive investment with increasing latitude and decreasing temperature may also be interpreted as local adaptation that generates CnGV in the sense of mitigating the decrease in fecundity due to the plastic decrease of energy acquisition. It results that higher latitudes and colder environments were also characterized by earlier maturation and stronger reproductive investment so that resulting adult size-at-age and asymptotic size followed a converse Bergmann's rule contrary to juvenile size-at-age. This highlights the complexity of predicting the result of local adaptation on a single trait, here size-at-age, when multivariate evolution of life-history traits – growth rate, maturation, reproductive investment – is involved.

The pattern observed across the studied sole populations reveals that local adaptation not only compensates but clearly overrides the plastic response to temperature. We might therefore assume either that CnGV is highly adaptive or that life history is affected by other factors than temperature that correlate with the latitudinal gradient, as physiological adaption to temperature is unlikely to be the only factor generating differences in life history between populations.

Adaptation to other gradient-related factors

As an alternative to highly adaptive CnGV in response to the temperature gradient, local adaptation along a gradient in natural mortality could be a plausible explanation. It is well known that both adults and juveniles of northern sole populations can suffer significantly elevated mortality rates during cold winters (Woodhead, 1964; Horwood and Millner, 1998). Environmentally induced mortality may increase variability in recruitment (Rijnsdorp et al., 1992), in line with the observed latitudinal trend in the coefficient of variation in recruitment from 19% in the Bay of Biscay to 90% in the North Sea (Table 2). Since size-independent mortality accelerates the pace of life history (Ernande et al., 2004; Jørgensen, 2013), it could be the main driver for the observed higher juvenile growth rates, earlier maturation and higher reproductive investment of northern populations. However, also negatively size-dependent mortality could induce higher juvenile growth rates but not earlier maturation (Abrams and Rowe 1996).

Differences in *per capita* food availability (including as a result of the effect of population density on growth) might also explain our results and would be reflected in the different estimates of the size-specific energy acquisition rate a. Since these estimates are higher for the northern populations, *per capita* food availability would have to be assumed higher in the north (Fig. 5). There is however no evidence for such pattern, as estimates for food availability are not available and exploitation rates, from which an effect of density-dependent growth could be inferred, have been similar across populations (see below).

The results of this study are thus in line with local adaptation either due to CnGV generated by physiological adaptation to temperature along the latitudinal gradient (CnGV; hypothesis H3 in Fig. 1C), or due to life-history adaptation to the latitudinal trend in natural mortality. This inference corroborates the results of population genetic studies using microsatellite

markers that revealed isolation by distance. The genetic structure reveals at least three different populations (Kattegat/Skagerrak region, the North Sea and the Bay of Biscay) and perhaps a fourth one in the Irish/Celtic Sea (Cuveliers et al., 2012). More recent ongoing studies using gene-linked SNP-markers suggest the presence of an even more fine-grained genetic structure, possibly due to local adaptations (G. Maes, pers. comm.).

Anthropogenic impacts?

There is evidence that exploited fish populations may adapt to human exploitation (Law and Grey, 1989; Heino & Godø, 2002; Jørgensen et al., 2007). As such, spatial differences in sole life-history could arise if exploitation was strongly heterogeneous spatially. In North Sea sole, females now mature at a younger age and smaller size than they did 4–5 decades ago, consistent with fisheries-induced evolution (Mollet et al., 2007). Differences in exploitation history therefore might have contributed to the presently observed differences in life-history traits among populations. Historically, sole had been exploited relatively lightly. The development of an intensive target fishery for sole began in the 1960s in the North Sea when vessels started using beam trawls rigged with heavy chains to chase sole up from the sea bed (Millner et al., 2005; Rijnsdorp et al., 2008). In the 1960s fishing mortality almost tripled from around 0.2 in the late 1950 to a level of 0.5–0.6 since 1970. Since the 1980s all populations have been exploited at fishing mortality rates between 0.4 and 0.6, except for 7e which had a fishing mortality rate of around 0.3 (ICES, 2010; Table 2). Given the rate of change in PMRN midpoints ascribed to fisheries-induced evolution (0.1 $cm.yr^{-1}$: Mollet et al., 2007), the amplitude of variation in the PMRN midpoints observed over the latitudinal gradient (about 5 cm: Fig. 8) could only arise from fisheries-induced evolution if exploitation rates differed extremely strongly between populations. Since exploitation rates were roughly similar across the latitudinal gradient, although they may have contributed to the observed

pattern, it appears unlikely that they could have been the main cause of the observed differences between populations.

Growth-independent temperature effect on PMRNs?

PMRNs disentangle the effects of environmental factors like temperature that act on maturation via variation in growth from the underlying (genetically determined) maturation process (Heino et al., 2002). However, temperature might also have a direct growth-independent effect on maturation probability: under warmer conditions, it has been reported that fish of a given age and size are more likely to mature by accelerating developmental rates (Kurita et al., 2003; Dhillon and Fox, 2004; Kuparinen et al., 2011, Neuheimer et al., 2012). Such growth-independent temperature effect would lead to a downward shift of the PMRN towards lower L_{P50} values in warmer areas (Grift et al., 2003; Mollet 2007). However, the differences in PMRNs found in this study were opposite to those expected from a growth-independent temperature effect: the cold-water populations were more likely to mature at a given age and size. Also condition and resource availability have been reported to explain variation in maturation probability additional to growth rates in terms of age and length (Grift et al., 2007, Uusi-Heikkilä et al., 2011). However, relating condition to maturation from wild capture data is uncertain because condition changes seasonally as a consequence of the annual process of reproduction: condition increases as an individual starts to store energy resources in somatic tissue for the subsequent spawning season and decreases as these resources are allocated to gonads that are subsequently spawned. Since maturity can be observed only as soon as energy resources have been allocated to gonads, the condition of an individual observed at this same moment is not a robust indicator for the likelihood of its maturity. Furthermore, condition may randomly vary on short time scales due to short-term changes in food availability (see discussion about *per capita* food availability above). If there

were persistent longer-term differences in *per capita* food availability between the populations it would likely also have induced a difference in average growth rates in terms of length, which would however have been captured by the PMRN. But there is no evidence to support any such speculations (see above). Given that the observed patterns were opposite to those expected from the major potential environmental effect for which there is evidence for differences between the environments of the here studied populations, i.e. temperature, we conclude that the population differences in PMRNs found in this study are likely of genetic nature.

Conclusions

We used a unique and novel approach to model growth and life history, which is more informative than the commonly used Von Bertalanffy growth model and overcomes the usual problems of biased sampling and size stratification in fisheries data. The approach has therefore the potential to become a standard application in fisheries science. For a meaningful analysis of this kind (also including the PMRN) an appropriate database of individual data is however crucial (see Fig. 1), and by combining data from three research institutions this paper represents a unique opportunity in this sense. Variation in life history between sole populations in the North-East Atlantic is found to be opposite to Bergmann's rule and thus neither the result of a phenotypically plastic response to temperature nor co-gradient adaptive variation. The observed pattern is consistent with local adaptation leading to countergradient variation. To our knowledge, this would be one of the first cases where CnGV is so strong that it does more than compensates for the plastic effects resulting from the temperature gradient, and thus leads to phenotypic variation opposite to the expectation from purely plastic variation. We hypothesise that other factors than temperature that are correlated with the latitudinal gradient must have played a role in overshooting the effect of CnGV. To our

current knowledge, strong latitudinal differences in natural mortality rates between populations offer the most plausible explanation for the life-history patterns observed in this study.

Acknowledgements

This research has been initially supported by the European Marie Curie Research Training Network FishACE (Fisheries-induced Adaptive Changes in Exploited Stocks, contract MRTN-CT-2004-005578) and was completed with support by the Specific Targeted Research Project FinE (Fisheries-induced Evolution, contract SSP-2006-044276) under the Scientific Support to Policies cross-cutting activities, both funded through the European Community's Sixth Framework Programme. It does not necessarily reflect the views of the European Commission and does not anticipate the Commission's future policy in this area. Additionally, GHE was supported by the UK Department for the Environment, Food and Rural Affairs (Defra) through projects MF1201 and MF1108 and ADR by the strategic research programme “Sustainable spatial development of ecosystems, landscapes, seas and regions” funded by the Dutch Ministry of Agriculture, Nature Conservation and Food Quality. BE thanks Gérard Biais for providing data and expertise on sole in the Bay of Biscay.

Cited Literature

Abookire, A.A., Macewicz, B.J. 2003. Latitudinal variation in reproductive biology and growth of female Dover sole (*Microstomus pacificus*) in the North Pacific, with emphasis on the Gulf of Alaska stock. *Journal of Sea Research* **50**, 187-197.

Abrams, P.A., Rowe, L. 1996. The effects of predation on the age and size of maturity of prey. *Evolution*, **50**, 1052–1061.

Angilletta, M.J. 2008. Thermal adaptation - a theoretical and empirical Synthesis. *Oxford University Press*.

Angilletta, M.J., Niewiarowski, P.H., Dunham, A.E., Leaché, A.D, Porter, W.P., 2004. Bergmann's clines in ectotherms: illustrating a life-history perspective with sceloporine lizards. *American Naturalist* **164**, 168-183.

Arbault, S., Camus, P., Lebec, C., 1986. Estimation of the common sole (*Solea vulgaris* Quensel 1806) spawning stock by egg survey in the Bay of Biscay. *Journal of Applied Ichthyology* **2**, 145-156.

Arendt, J.D., 1997. Adaptive intrinsic growth rates: an integration across taxa. *The Quarterly Review of Biology* **72**, 149-177.

Arnett, A.E., Gotelli, N.J., Url, S., 1999. Geographic variation in life-history traits of the ant lion, *Myrmeleon immaculatus*: evolutionary implications of Bergmann's Rule. *Evolution* **53**, 1180-1188.

Atkinson, D., Sibly, R.M., 1997. Why are organisms usually bigger in colder environments? Making sense of a life history puzzle. *Trends in Ecology and Evolution*, **12**, 235–239.

Barot, S., Heino, M., O'Brien, L., Dieckmann, U., 2004. Estimating reaction norms for age and size at maturation when age at first reproduction is unknown. *Evolutionary Ecology Research* **6**, 659-678.

Bergmann, C., 1847. Über die Verhältnisse der Wärmeökonomie der Thiere zu ihrer Grösse. *Göttinger Studien* **3**, 595-708.

Bernardo, J., 1993. Determinants of maturation in animals. *Trends in Ecology and Evolution* **8**, 166-173.

Blackburn, T.M., Hawkins, B.A., 2004. Bergmann's rule and the mammal fauna of northern North America. *Ecography* **27**, 715-724.

Blanckenhorn, W.U., Demont, M.D., 2004. Bergmann and converse Bergmann latitudinal clines in arthropods: two ends of a continuum? *Integrative and Comparative Biology* **44**, 413-424.

Brander, K.M., 2007. The role of growth changes in the decline and recovery of North Atlantic cod stocks since 1970. *ICES Journal of Marine Science* **64**, 211-217.

Brunel. T., Dickey-Collas, M., 2010. Effects of temperature and population density on von Bertalanffy growth parameters in Atlantic herring: a macro ecological analysis. *Marine Ecology Progress Series*, **405**, 15-28.

Brunel, T., Ernande, B., Mollet, F.M., Rijnsdorp, A.D. 2013. Coupling non-linear mixed statistical models and dynamic energy allocation models to determine the onset of maturation and related energy allocation parameters from somatic growth data. Oecologia, in press.

Conover, D.O., Duffy, T.A., Hice, L.A., 2009. The covariance between genetic and environmental influences across ecological gradients - reassessing the evolutionary significance of countergradient and cogradient Variation. *The Year in Evolutionary Biology* **Ann. N. Y.,** 100-129.

Conover, D.O., Present, T.M.C., 1990. Countergradient variation in growth rate - compensation for length of the growing season among Atlantic silversides from different latitudes. *Oecologia* **83**, 316-324.

Conover, D.O. Schultz, E.T., 1995 Phenotypic similarity and the evolutionary significance of countergradient variation. *Trends in Ecology and Evolution* **10**, 248–252. (doi:10.1016/S0169-5347(00)89081-3)

Cuveliers, E., Larmuseau, M., Hellemans, B., Verherstraeten, S., Volckaert, F., Maes, G., 2012. Multi-marker estimate of genetic connectivity of sole (*Solea solea*) in the North-East Atlantic Ocean. *Marine Biology* **159**, 1239-1253. doi: 10.1007/s00227-012-1905-x

Deniel, C., 1981. , pleuronectiformes) en Baie de Douarnenez: reproduction, croissance et migration des Bothidae, Scophthalmidae, Pleuronectidae et Soleidae. **PhD thesis**, .

Dhillon, R.S., Fox, M.G., 2004. Growth-independent effects of temperature on age and size at maturity in Japanese medaka (*Oryzias latipes*). *Copeia* **2004**, 37−45.

Engelhard, G.H., Heino, M., 2004. Maturity changes in Norwegian spring spawning herring before, during, and after a major population collapse. *Fisheries Research* **66**, 299-310.

Ernande B., Dieckmann, U., Heino, M. 2004. Adaptive changes in harvested populations: plasticity and evolution of age and size at maturation. *Proceedings of the Royal Society B Biological Sciences* **271**, 415-423.

Exadactylos, A., Geffen, A.J., Panagiotaki, P., Thorpe, J.P., 2003. Population structure of Dover sole *Solea solea*: RAPD and allozyme data indicate divergence in European stocks. *Marine Ecology Progress Series* **246**, 253-264.

Fincham, J.I., Rijnsdorp, A.D., Engelhard, G.H., 2013. Shifts in the timing of spawning in sole linked to warming sea temperatures. *Journal of Sea Research* **75**, 69-76. doi:10.1016/j.seares.2012.07.004

Fonds, M., Cronie, R., Vethaak, A.D., Van Der Puyl, P., 1992. Metabolism, food consumption and growth of plaice (*Pleuronectes platessa*) and flounder (*Platichthys flesus*) in relation to fish size and temperature. *Netherlands Journal of Sea Research* **29**, 127-143.

Fox, C.J., O'Brien, C.M., Dickey-Collas, M., Nash, R.D.M., 2000. Patterns in the spawning of cod (*Gadus morhua* L.), sole (*Solea solea* L.) and plaice (*Pleuronectes platessa* L.) in the Irish Sea as determined by generalized additive modelling. *Fisheries Oceanography* **9**, 33-49.

Gardner, J.L., Heinsohn, R., Joseph, L., 2009. Shifting latitudinal clines in avian body size correlate with global warming in Australian passerines. *Proceedings of the Royal Society B Biological Sciences* **276**, 3845-3852.

Grift, R.E., Rijnsdorp, A.D., Barot, S., Heino, M., Dieckmann, U., 2003. Fisheries-induced trends in reaction norms for maturation in North Sea plaice. *Marine Ecology Progress Series* **257**, 247-257.

Grift, R.E., Heino, M., Rijnsdorp, A.D., Kraak, S.B.M., Dieckmann, U., 2007. Three-dimensional maturation reaction norms for North Sea plaice. *Marine Ecology Progress Series* **334**, 213–224.

Heino, M., Dieckmann, U., Godo, O.R. 2002. Measuring probabilistic reaction norms for age and size at maturation. *Evolution* **56**, 669-678.

Heino, M., Godø, O.R., 2002. Fisheries-induced selection pressures in the context of sustainable fisheries. Bulletin of Marine Science 70, 639–656.

Horwood, J., 1993. The Bristol Channel sole (*Solea solea* (L.)) - a fisheries case-study. Advances in Marine Biology **29**, 215-367.

Horwood, J.W., Millner, R.S., 1998. Cold induced abnormal catches of sole. *Journal of the Marine Biological Association of the United Kingdom* **78**, 345–347.

Huret, M., Sourisseau, M., Petitgas, P., Struski, C., Léger, F., Lazure, P., 2013. A multi-decadal hindcast of a physical–biogeochemical model and derived oceanographic indices in the Bay of Biscay. Journal of Marine Systems. dx.doi.org/10.1016/j.jmarsys.2012.02.009.

ICES, 2010. Report of the ICES Advisory Committee 2010. ICES Advice, 2010. Book 6, 309 pp.

Jørgensen, C., Enberg, K., Dunlop, E. S., Arlinghaus, R., Boukal, D.S., Brander, K., Ernande, B., Gårdmark, A., Johnston, F., Matsumura, S., Pardoe, H., Raab, K., Silva, A., Vainikka, A., Dieckmann, U., Heino, M., Rijnsdorp, A.D., 2007. Managing evolving fish stocks. *Science* **318**, 1247-1248.

Jørgensen, C., Holt, R.E., 2013. Natural mortality: its ecology, how it shapes fish life histories, and why it may be increased by fishing. *Journal of Sea Research* **75**, 8-18.

Jørgensen, T., 1990. Long-term changes in age at sexual maturity of Northeast Arctic cod (*Gadus morhua* L.). *Journal du Conseil International pour l'Exploration de la Mer* **46**, 235-248.

Kuparinen, A., Cano, J.M., Loehr, J., Herczeg, G., Gonda, A., Merilä, J., 2011. Fish age at maturation is influenced by temperature independently of growth. *Oecologia* **167**, 435-443.

Kurita, Y., Meier, S., Kjesbu, O.S., 2003. Oocyte growth and fecundity regulation by atresia of Atlantic herring (*Clupea harengus*) in relation to body condition throughout the maturation cycle. *Journal of Sea Research* **49**, 203-219.

Laugen, A.T., Laurila, A., Räsänen, K., Merilä, J., 2003. Latitudinal countergradient variation in the common frog (*Rana temporaria*) development rates - evidence for local adaptation. *Journal of Evolutionary Biology* **16**, 996-1005.

Laugen, A.T., Laurila, A., Jonsson, K., Soderman, F., Merilä, J., 2005. Do common frogs (*Rana temporaria*) follow Bergmann's rule? *Evolutionary Ecology Research* **7**, 717-731.

Law, R., Grey, D.R., 1989. Evolution of yields from populations with age-specific cropping. *Evolutionary Ecology* **3**, 343-359.

Lester, N.P., Shuter, B.J., Abrams, P.A., 2004. Interpreting the von Bertalanffy model of somatic growth in fishes: the cost of reproduction. *Proceedings of the Royal Society of London Series B Biological Sciences* **271**, 1625-1631.

Lindgren, B., Laurila, A. 2005. Proximate causes of adaptive growth rates: growth efficiency variation among latitudinal populations of Rana temporaria. *Journal of Evolutionary Biology* **18**, 820-828.

Lindgren, B., Laurila, A. 2010. Are high-latitude individuals superior competitors? A test with *Rana temporaria tadpoles*. *Evolutionary Ecology* **24**, 115-131.

Lynch, M., Walsh, B. 1998. *Genetics and Analysis of Quantitative Traits*. Sinauer Associates.

Litzgus, J.D., Durant, S.E., Mousseau, T.A., 2004. Clinal variation in body and cell size in a widely distributed vertebrate ectotherm. *Oecologia* **140**, 551-558.

Lonsdale, D.J., Levinton, J.S., 2011. Latitudinal differentiation in copepod growth: an adaptation to temperature. *Ecology* **66**, 1397-1407.

Marcil, J., Swain, D.P., Hutchings, J.A., 2006. Countergradient variation in body shape between two populations of Atlantic cod (*Gadus morhua*). *Proceedings of the Royal Society B Biological Sciences* **273**, 217-223.

Millner, R.S., Walsh, S.J., Diaz de Asarloa, J.M., 2005. Atlantic flatfish fisheries. In: Gibson, R.N. (Ed.), Flatfishes: Biology and exploitation. *Blackwell Science Ltd*, Oxford, UK, pp. 240-271

Mollet, F.M., Ernande, B., Brunel, T., Rijnsdorp, A.D., 2010. Multiple growth-correlated life history traits estimated simultaneously in individuals. *Oikos* **119**, 10-26.

Mollet, F.M., Kraak, S.B.M., Rijnsdorp, A.D., 2007. Fisheries-induced evolutionary changes in maturation reaction norms in North Sea sole *Solea solea*. *Marine Ecology Progress Series* **351**, 189-199.

Mousseau, T.A., 1997. Ectotherms follow the converse to Bergmann's rule. *Evolution* **51**, 630-632.

Neuheimer, A.B., Grønkjaer, P., 2012. Climate effects on size-at-age: growth in warming waters compensates for earlier maturity in an exploited marine fish. *Global Change Biology* **18**,1812–1822.

O'Brien, L., 1999. Factors influencing the rate of sexual maturity and the effect on spawning stock for Georges Bank and Gulf of Maine Atlantic cod *Gadus morhua* stocks. *Journal of Northwest Atlantic Fisheries Science* **25**, 179-203.

Partridge, L., Coyne, J.A., 1997. Bergmann's rule in ectotherms: is it adaptive? *Evolution* **51**, 632-635.

Pinheiro, J.C., Bates, D.M., 2004. Mixed-Effects Models in S and S-PLUS. Statistics and Computing. *Springer, New York, USA*, 528 pp.

Pinheiro, J., Bates, D., DebRoy, S., Sarkar, D., and the R Development Core Team. 2011. nlme: Linear and Nonlinear Mixed Effect Models. R package version 3.1-102

R Development Core Team. 2011. R: A language and environment for statistical computing. R Foundation for Statistical Computing, Vienna, Austria.

Rijnsdorp, A.D., 1990. The mechanism of energy allocation over reproduction and somatic growth in female North Sea plaice, *Pleuronectes platessa* L. *Netherlands Journal of Sea Research* **25**, 279-289.

Rijnsdorp, A.D., Van Beek, F.A., Flatman, S., Millner, R., Giret, M., De Clerck, R., 1992. Recruitment of sole stocks, Solea solea (L.), in the northeast Atlantic. *Netherlands Journal of Sea Research* **29**, 173-192.

Rijnsdorp, A.D., Vingerhoed, B., 1994. The ecological significance of geographical and seasonal differences in egg size in sole *Solea solea* (L.). *Netherlands Journal of Sea Research* **32**, 255-270.

Rijnsdorp, A.D., Witthames, P., 2005. Ecology of reproduction. In Gibson, R.N. (Ed.), *Flatfishes: Biology and Exploitation*. Blackwell Science, Oxford, UK, pp. 68-93.

Rijnsdorp, A.D., Poos, J.J., Quirijns, F.J., HilleRisLambers, R., de Wilde, J.W., Den Heijer, W.M., 2008. The arms race between fishers. *Journal of Sea Research* **60**, 126–138

Roff, D.A., 1992. *The evolution of life histories*. New York: Chapman & Hall.

Schultz, E.T., Reynolds, K.E., Conover, D.O., 1996. Countergradient variation in growth among newly hatched *Fundulus heteroclitus*: geographic differences revealed by common-environment experiments. *Functional Ecology* **10**, 366-374.

Skelly, D.K., 2004. Microgeographic countergradient variation in the Wood Frog, *Rana sylvatica*. *Evolution* **58**, 160-165.

Stearns, S.C., 1992. *The evolution of life histories*. New York: Oxford University Press.

Søiland, H., Skogen, M.D., 2000. Validation of a three-dimensional biophysical model using nutrient observations in the North Sea. *ICES Journal of Marine Science* **57**, 816-823.

Toresen, R., 1990. Long term changes in growth of Norwegian spring spawning herring. *Journal du Conseil International pour l'Exploration de la Mer* **47**, 48–56.

Trussell, G.C., 2000. Phenotypic clines, plasticity, and morphological trade-offs in an intertidal snail. *Evolution* **54**, 151-166.

Trussell, G.C., 2002. Evidence of countergradient variation in the growth of an intertidal snail in response to water velocity. *Marine Ecology Progress Series* **243**, 123-131.

Uusi-Heikkilä, S., Kuparinen, A., Wolter, C., Meinelt, T., O'Toole, A.C.O., Arlinghaus, R., 2011. Experimental assessment of the probabilistic maturation reaction norm: condition matters. *Proceedings of the Royal Society B Biological Sciences* **278**, 709–17.

Vainikka, A., Mollet, F., Casini, M., Gårdmark, A., 2009: Spatial variation in growth, condition and maturation reaction norms of the Baltic herring (*Clupea harengus membras*). *Marine Ecology Progress Series* **383**, 285-294.

Van Voorhies, W.A., 1997. On the adaptive nature of Bergmann size clines: a reply to Mousseau, Partridge and Coyne. *Evolution* **51**, 635-640.

West, G.B., Brown, J.H., Enquist, B.J., 2001. A general model for ontogenetic growth. *Nature* **413**, 628-631.

Witthames, P.R., Walker, M.G., Dinis, M.T., Whiting, C.L., 1995. The geographical variation in the potential annual fecundity of Dover sole *Solea solea* (L) from European shelf waters during 1991. *Netherlands Journal of Sea Research* **34**, 45-58.

Woodhead, P.J.M., 1964. The death of North Sea fish during the winter of 1962/63 particularly with reference to the sole, *Solea vulgaris*. *Helgoländer Wissenschaftliche Meeresuntersuchungen* **10**, 283–300.

Tables & Figures

Table 1: Sample numbers per area and age group, number of data points (individuals) used in growth (#growth) and maturation (#mature) analysis and the proportion of matures (%mature) at age (referring to the age at spawning). The differences between the growth and maturity data selection arises because maturity, in contrast to size and age, is not routinely assessed in surveys. The proportion of mature individuals at age is not representative of maturity ogives because the size distribution in each age class is biased due to length-stratified sampling and minimal mesh and landing size regulations (especially affecting size distributions in younger age classes).

area	Count (#) or percentage (%)	age1	age2	age3	age4	age5	age6	age7+	total
8a	#growth	32	386	602	673	589	410	770	3462
	#mature	4	99	107	159	166	134	270	939
	%mature	0.00	0.01	0.15	0.63	0.80	0.84	0.92	0.65
7e	#growth	34	167	567	660	476	294	636	2834
	#mature	0	22	283	328	151	155	288	1227
	%mature	NA	0.14	0.71	0.94	0.99	0.99	1.00	0.90
7d	#growth	565	2390	2668	2365	1664	910	2103	12670
	#mature	4	161	844	808	562	354	877	3610
	%mature	0.75	0.13	0.60	0.82	0.81	0.84	0.92	0.76
7fg	#growth	510	776	335	316	395	214	511	3116
	#mature	0	1	15	58	87	87	192	440
	%mature	NA	0.00	0.53	0.93	0.98	0.99	1.00	0.97
4c	#growth	789	1968	4299	4696	3733	1935	3940	21458
	#mature	10	179	1275	1411	1085	615	1071	5646
	%mature	0.00	0.38	0.93	0.96	0.94	0.96	0.92	0.92
4bW	#growth	1	114	261	195	156	141	194	1062
	#mature	0	19	105	95	83	66	87	455
	%mature	NA	0.26	0.80	0.93	1.00	1.00	1.00	0.91
7a	#growth	274	629	523	540	367	192	397	2928
	#mature	0	0	19	48	56	23	98	244
	%mature	NA	NA	1.00	0.96	1.00	1.00	1.00	0.99
4bE	#growth	269	975	2064	2291	1349	803	1048	8850
	#mature	0	72	695	922	560	341	471	3061
	%mature	NA	0.50	0.95	0.99	1.00	1.00	1.00	0.97
total	#growth	2474	7405	11319	11736	8729	4899	9599	56380
	#mature	2474	7405	11319	11736	8729	4899	3354	15622
	%mature	0.17	0.24	0.80	0.92	0.92	0.94	0.95	0.88

Table 2: Environmental conditions and estimated growth parameters and derived quantities (see text) for each stock based on random effects estimated in the random area effect model (eq. 4). Mean latitude and temperature as described in text; CV recruitment: coefficient of variation of the number of recruits over the last 25 - 50 years (periods of available data differ between areas) from Rijnsdorp & Witthames (2005); *Mean F*: mean fishing mortality, fishing mortality data from ICES Fish Stock Assessment Summary Database (2010); a: size-specific energy acquisition rate, c: size-specific reproductive investment rate; w_{mat}: weight at maturation; t_{mat}: age at maturation; L_{P50}: PMRN midpoint at age 3; W_{P50}: weight corresponding to PMRN midpoint at age 3; L_{∞}: asymptotic length; W_{∞}: asymptotic weight; $se(x)$: standard error of estimate x obtained by bootstrapping.

Stock	**8a**	**7e**	**7d**	**7fg**	**4c**	**4bW**	**7a**	**4bE**
Latitude [°N]	47	49.7	50.5	51.4	51.7	53.5	54	54.5
Temperature [°C]	13.6	11.8	11.8	11.1	11.3	9.5	10.6	9.8
Day of peak spawning	58	91	111	86	118	151	136	148
***CV* Recruitment**	19%	36%	38%	43%	90%[1]	90%[1]	75%	90%[1]
***Mean F*[2]**	0.515	0.339	0.424	0.482	0.541	0.541	0.483	0.541
***a* [$g^{1/4}yr^{-1}$]**	4.55	5.10	5.17	5.61	5.26	4.59	5.16	5.89
***se*(*a*) [$g^{1/4}yr^{-1}$]**	0.09	0.40	0.21	0.14	0.07	0.23	0.09	0.07
***c* [yr^{-1}]**	0.678	0.870	0.904	1.000	0.904	0.776	0.942	1.042
***se*(*c*) [yr^{-1}]**	0.025	0.083	0.052	0.038	0.017	0.053	0.024	0.018
w_{mat} [g]	117	129	119	68	49	118	81	67
$se(w_{mat})$ [g]	6.90	38.47	12.21	4.37	4.42	19.20	4.00	3.19
t_{mat} [yr]	2.54	2.34	2.25	1.76	1.72	2.53	2.02	1.67
$se(t_{mat})$ [yr]	0.09	0.38	0.15	0.08	0.07	0.23	0.06	0.04
L_{P50} [cm]	27.8	24.3	25.3	26.3	24.1	25.2	23.2	22.9
W_{P50} [g]	185	146	170	178	133	130	172	97
L_{∞} [cm]	57.56	48.26	47.21	46.15	49.62	50.50	44.89	48.00
$se(L_{\infty})$ [cm]	1.19	1.06	0.82	0.86	0.36	1.15	0.56	0.31
W_{∞} [g]	2031	1175	1071	993	1142	1222	899	1023
$se(W_{\infty})$ [g]	130	81	55	60	26	87	34	21

[1] Recruitment variability for total North Sea stock (4c, 4bW, 4bE combined).

[2]Mean F for the years 1984–2007, averaged over ages 3–6 (area 8a), 3–7 (7e), 3–8 (7d), 4–8 (7fg), 4–7 (Irish Sea), and 2–6 (4c, 4bW, 4bE).

Table 3: Comparison of the performance of the three nonlinear mixed effect models. Random area effect model: model with constant fixed effects and area random effects acting on the three parameters (a, c, w_{mat}) with a symmetric covariance matrix; Latitude effect model: model with fixed effects depending linearly on area average latitude and area random effects on parameter a and w_{mat} with a symmetric covariance matrix; Temperature effect model: model with fixed effects depending linearly on area average temperature and area random effects on parameter a and w_{mat} with a diagonal covariance matrix. Number of parameters (n), Akaike Information Criterion (AIC), Bayesian Information Criterion (BIC) and log(likelihood) are given for each model.

Model	**n**	**AIC**	**BIC**	**log(likelihood)**
Random area effect model	17	-7067.5	-6915.5	3550.7
Latitude effect model	17	-7081.7	-6929.7	3557.8
Temperature effect model	16	-7134.3	-6991.3	3583.2

Table 4: Detailed effects of latitude or temperature on the three parameters of the growth model, namely size-specific energy acquisition a, size-specific reproductive investment c and weight at maturation w_{mat}. For each parameter, subscripts 0 and 1 refer respectively to the intercept and the slope of the linear dependency on latitude (Lat) or temperature ($\overline{T}$) (eq. 5) in the corresponding fixed effect model (eq. 4). Estimate and standard error (s.e.) are given for each parameter together with the degrees of freedom (df), t-value and associated p-value testing for its significance.

Parameter	Estimate	s.e.	df	t-value	p-value
Latitude effect model					
a_{0,Lat_z}	4.61	0.10	56367	46.37	<0.0001
a_{1,Lat_z}	0.15	0.20	56367	7.68	<0.0001
c_{0,Lat_z}	0.717	0.011	56367	66.19	<0.0001
c_{1,Lat_z}	0.045	0.002	56367	20.74	<0.0001
$w_{\text{mat},0,Lat_z}$	129	22.58	56367	5.71	<0.0001
$w_{\text{mat},1,Lat_z}$	-9	4.40	56367	-2.14	0.0327
Temperature effect model					
$a_{0,\overline{T}_z}$	5.86	0.09	56367	67.78	<0.0001
$a_{1,\overline{T}_z}$	-0.28	0.04	56367	-6.62	<0.0001
$c_{0,\overline{T}_z}$	1.076	0.010	56367	102.68	<0.0001
$c_{1,\overline{T}_z}$	-0.081	0.005	56367	-15.49	<0.0001
$w_{\text{mat},0,\overline{T}_z}$	51	15.94	56367	3.20	0.0014
$w_{\text{mat},1,\overline{T}_z}$	17	7.92	56367	2.16	0.0310

Table 5: Randomization tests for pairwise differences in PMRN between areas. p-values give the likelihood that the difference between two stocks arises by chance only, based on 10^4 repetitions of the PMRN midpoints calculation after randomizing subpopulations. Differences in PMRN midpoints between subpopulations for which this likelihood is higher than 5% are given in bold.

8a								
7e	0.000							
7d	0.000	0.004						
7fg	0.019	0.002	0.015					
4c	0.000	**0.093**	0.000	0.000				
4bW	0.000	0.049	**0.390**	0.045	0.002			
7a	0.004	**0.072**	0.022	0.011	**0.121**	0.028		
4bE	0.000	0.000	0.000	0.000	0.000	0.000	**0.378**	
	8a	**7e**	**7d**	**7fg**	**4c**	**4bW**	**7a**	**4bE**

Figure 1: Possible latitudinal clines in phenotypic expression and their underlying genetic and environmental causes (modified from Conover and Schultz, 1995; Conover et al., 2009). In this example temperature decreases with latitude (see Fig. 3), and we use growth rate as an example of phenotype. In ectotherms such as fish, lower temperature generally slows down physiological rates (solid line), but the resulting phenotype (dashed line) also depend on the genetic influence (dotted line) and the interaction between the environmental and the genetic processes along the gradient.

A: There is no genetic variation for growth between populations along the gradient, and the resulting phenotypic variation is determined by the change in environmental conditions (phenotypic expression – dashed line – coincides with environmental influence – solid line).

B: The genotypic influence on a trait along the gradient is positively correlated to environmental influence on a trait along a gradient. For growth rate this will occur if there is selection for fast growth in an environment that favours growth (e.g. high temperature) and *vice versa*. Morphological characters have often been found to display CoGV (Conover et al., 2009)

C: The genotypic influence on a trait along the gradient opposes the environmental influence on a trait along the gradient. For growth this will occur if there is strong selection for faster growth in environments that tend to slow down growth (e.g. low temperature, restricted growth season, see e.g. Laugen et al., 2003).

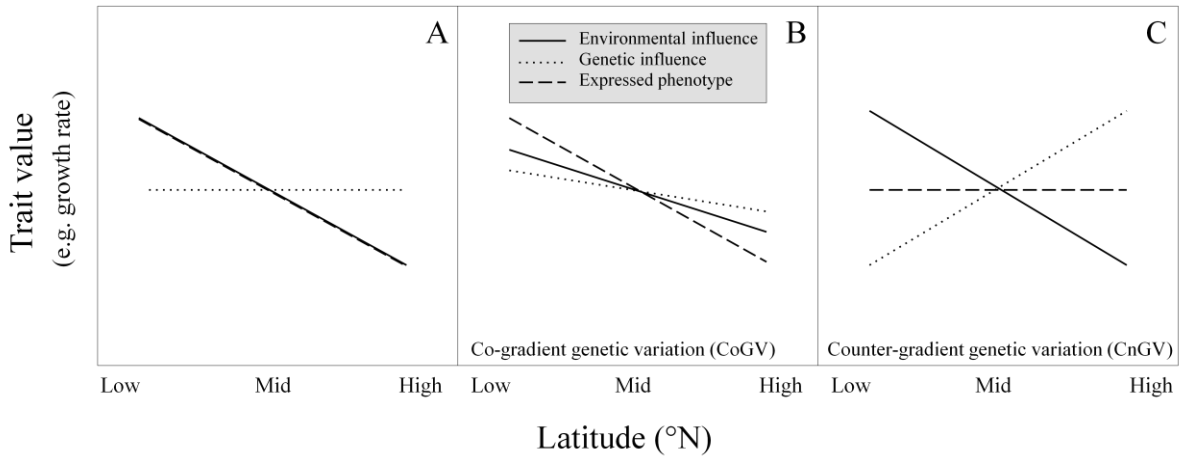

Figure 2: Geographic distribution of the study sole populations. Map showing the definition of eight ICES fishing regions, corresponding approximately with the distribution ranges for eight sole populations distinguished here. Shaded areas illustrate the locations of major sole spawning grounds schematically (based on Arbault et al., 1986; Rijnsdorp et al., 1992; Fox et al., 2000).

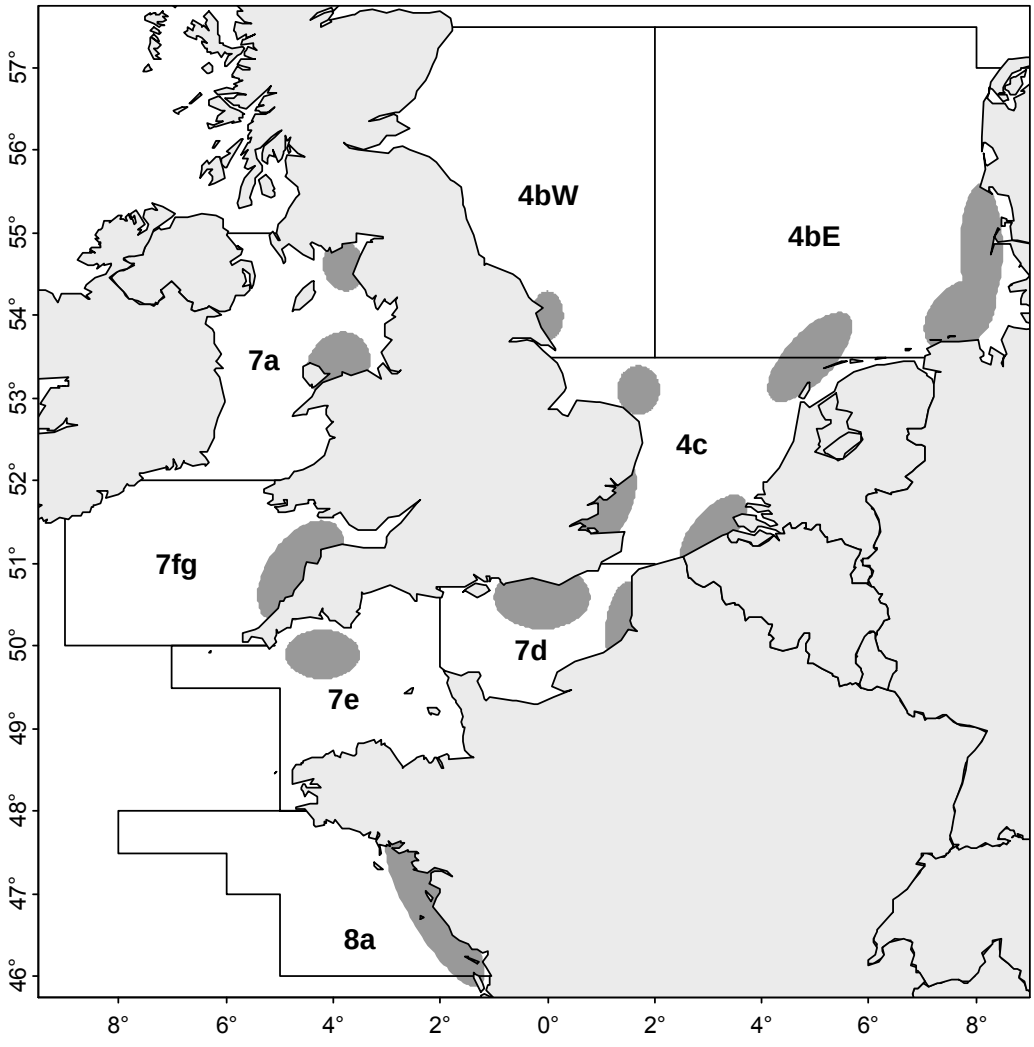

Figure 3: Latitudinal clines in sea bottom temperature and spawning timing of sole. Relationship between latitude and bottom temperature (from a biophysical model: NORWECOM, IMR; and hydro-dynamical model MARS3D, IFREMER, see text) for the different study populations (upper panel). Symbols indicate the annual mean, and bars the minimum and maximum temperatures throughout the year. Relationship of latitude with peak spawning day (filled circles) as suggested by literature for the different study populations of sole, and the spawning low (open circles) as estimated from the minimal condition in the seasonal cycle (see eq. 6, predicted for a body length of 35cm, lower panel). Days are Julian dates referring to the 1st of January as start of the year. The dotted lines represent linear regressions of the thereby approximated start and end of spawning weighted by the number of observations in each stock.

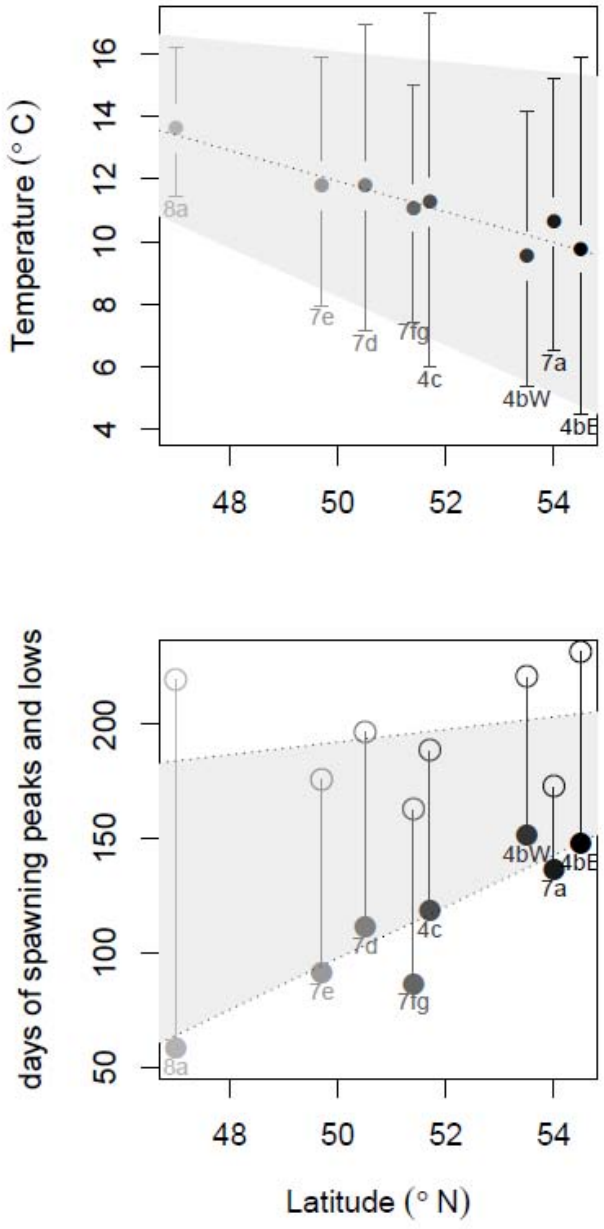

Figure 4: Latitudinal cline in growth curves. Age at weight data with means and 95% confidence interval bars for ages within each size class (10 g) and fitted growth curves from the selected model with lowest AIC (temperature effect model, see Table 2 & 3) are presented for the eight stocks analyzed ordered according to increasing average latitude (solid line).

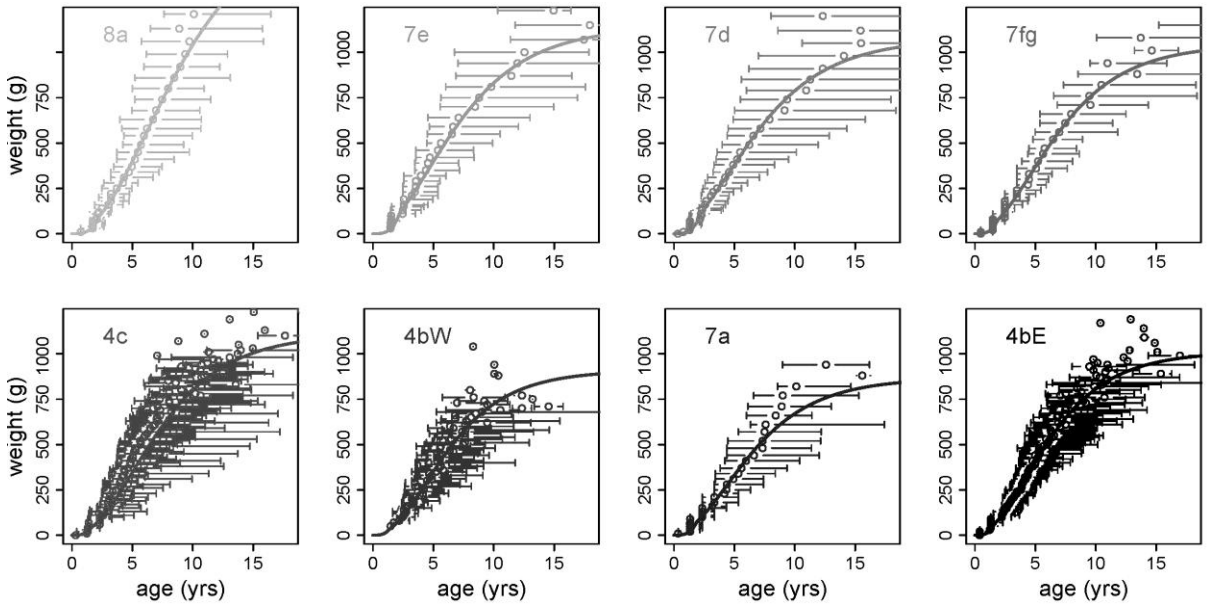

Figure 5: Latitudinal and temperature-related phenotypic clines in life-history parameters of the energy allocation model. The three fitted energy allocation parameters, energy acquisition rate a, reproductive investment rate c, onset of maturation w_{mat} for each stock (see $\boldsymbol{\mu}(x_z)+\Delta\boldsymbol{\mu}_z$ in eq. 4) and the underlying temperature effect on the fixed effects across stocks (dotted line, see $\boldsymbol{\mu}(x_z)$ in eq. 4) of the temperature effect model (upper panel) and the latitude effect model (lower panel, see corresponding values in Table 4).

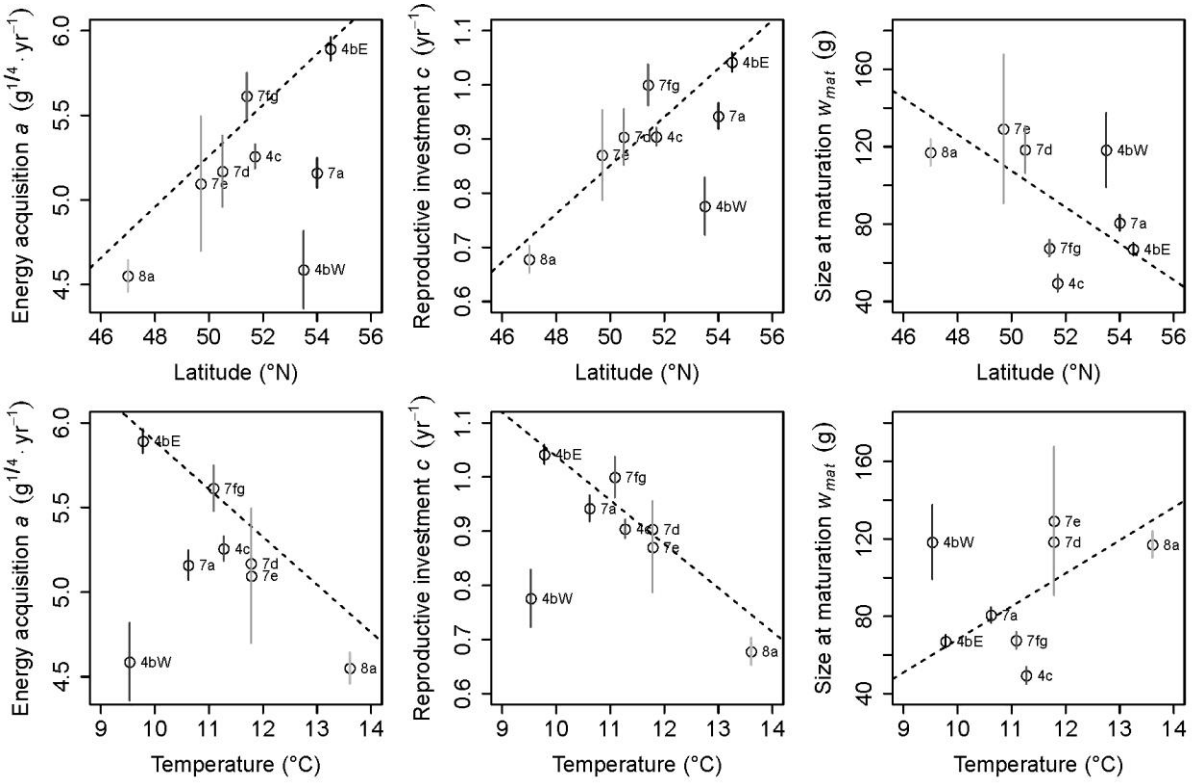

Figure 6: Temperature-related phenotypic clines in derived life-history traits. Age at maturation t_{mat}, asymptotic weight w_{inf}, average size at age 2, 3, 4, and 5 as predicted from the growth models for each area or subpopulation are presented as functions of average temperature (open circles) with linear regression on temperature (dashed line). Before maturation northern populations tend to display larger size at age but this pattern changes after maturation.

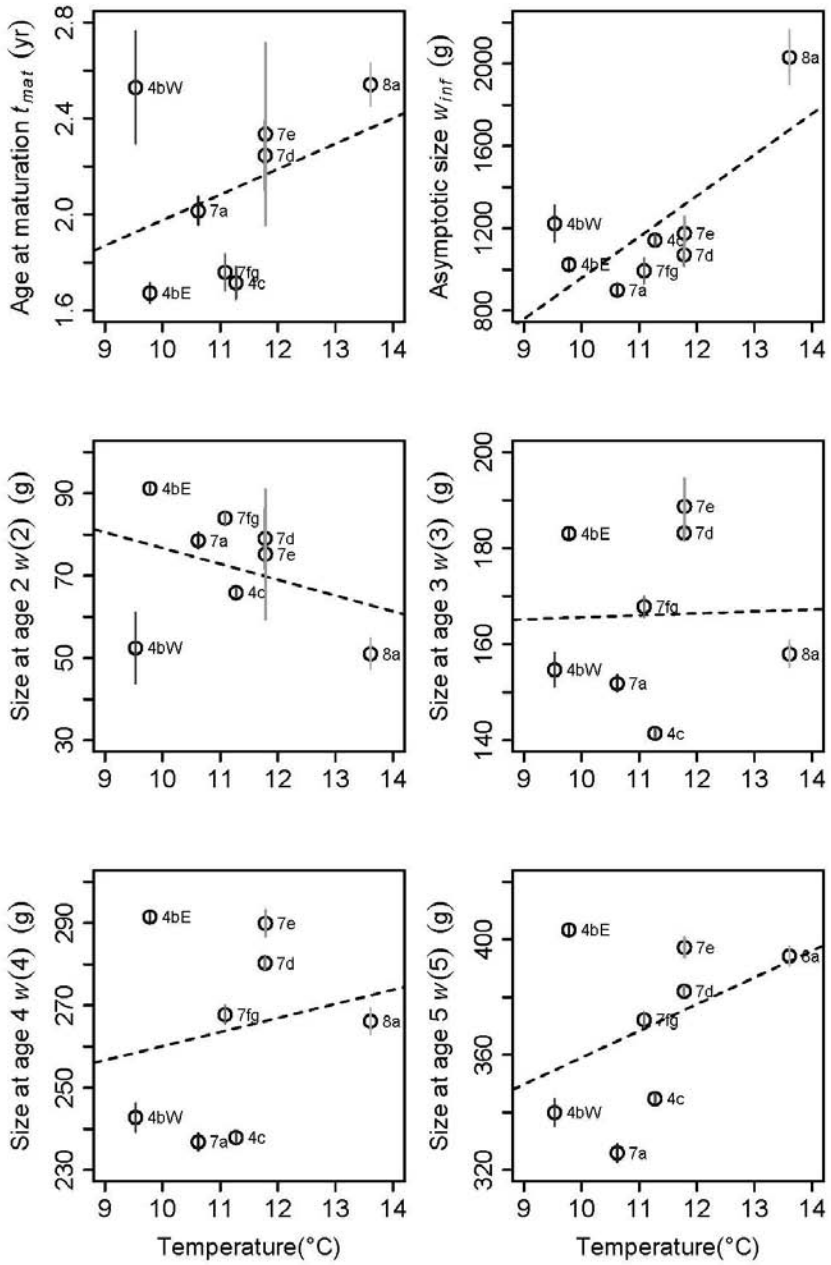

Figure 7: PMRNs in length (cm) for the 50% probability of maturing as a function of age for the 8 studied areas, each representing a subpopulation. For illustration purposes the PMRNs are shown over a large age-size spectrum, however only ages 2-4 years and sizes 18-32cm occur and are relevant for growth and maturation (indicated by gray shadings), and represent the age-size spectrum where observations come from. The rest of the lines represent extrapolations of the PMRN model.

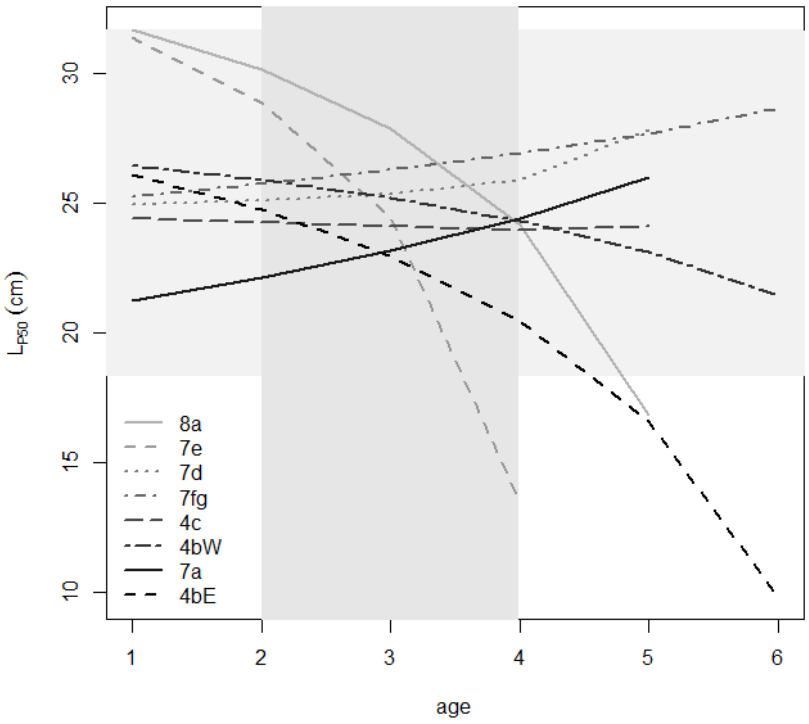

Figure 8: PMRN L_{P50} midpoints at age 3, the age at which most individuals become mature, as a function of temperature (left panel) and latitude (right panel) with upper and lower 95%-confidence intervals obtained by bootstrapping the data in each area for the PMRN analysis in 10^4 replicates. The regression of the L_{P50} midpoints on average temperature (dashed line) was weighted by the inverse of the bootstrapped variance and is for temperature significant on a level of α=0.103, for latitude on a level of α=0.025.